Orissa Journal of Physics
ISSN 0974-8202

Vol. 31, No.1
February 2024
pp. 5-14

Intrinsic Shear and Galaxy Alignments: A Quantitative Study Using the TATT model

A. DAS

Department of Astronomy, Steward Observatory,
The University of Arizona, 933 N Cherry Ave,
Tucson, AZ 85719, United States

Received 11.11.23, Accepted 31.12.23

Abstract : The intrinsic alignment (IA) of galaxies acts as a systematic effect in weak lensing measurements and tends to introduce biases. It mimics the gravitational lensing signal which makes it difficult to distinguish it from the true gravitational weak lensing effect. Hence, it is critical to account for the noise for correctly interpreting the results. This study aims at a quantitative analysis of IA using the Tidal Alignment and Tidal Torquing (TATT) model. We also investigate how the signals for shear and galaxy-galaxy lensing behave upon changing the parameters of the TATT model. The data for this study was prepared with a computational pipeline based on the Cocoa model to explore the parameter space of the intrinsic shape signal. Through this work, we identify that linear terms of the intrinsic shape signal are dominant in the case of GGL while the higher-order terms dictate the shear signal.

Keywords: Intrinsic Alignments, Weak Gravitational Lensing, Tidal Alignment, Tidal Torquing, Cosmic Shear, Galaxy Alignments

1. Introduction

The intrinsic alignment of galaxies is the correlation of galaxy shapes and orientations to nearby galaxies and underlying dark matter distribution (Joachimi et al. 2015; Bhowmick et al. 2019). It allows us to understand the evolutionary history of galaxies and the nature of dark energy. However, IA is a source of systematic error in weak gravitational lensing (WL) measurements (Troxel & Ishak 2014; Joachimi et al. 2015).

Weak gravitational lensing is the phenomenon in which foreground galaxies

and other large-scale structures distort the images of background galaxies because of their gravitational shear. Statistical analysis of their correlations carries information about the large-scale structure of the universe. Therefore, these weak lensing signals have emerged as probes for studying cosmic structures, distribution of underlying dark matter, and for studying different expansion models of the universe (Brainerd et al. 1996).

Nevertheless, the precision with which we can measure the weak lensing signal depends on how well we can differen- tiate the IA signal from it. And, to address the issue of intrinsic alignment an in-depth understanding of galaxy bias and tidal fields is warranted (Mandelbaum 2018)

The Tidal Alignment and Tidal Torquing Model first proposed by Blazek et al. (2019) incorporates both the tidal forces that affect the alignment of galaxies and the tidal torque for the angular momentum dependent pro- cesses.(Lamman et al. 2023). In this work, we investigate how efficient is the TATT model in describing the intrinsic alignment of galaxies.

2. Theoretical Background

Intrinsic Alignments are non-random orientations of the galaxies relative to the large-scale structures of the Universe as a consequence of the gravitational interactions and the anisotropic nature of structure formation (Kiessling et al. 2015). The tidal torque theory forms the theoretical foundations for IA, that states angular momentum of a galaxy is influenced by the tidal forces exerted by the underlying matter distribution during the formation of the galaxy and the alignment of galaxies in their clusters is the result of asymmetric cluster formation (Doroshkevich 1970; Wesson 1984). The IA of elliptical galaxies is under the influence of tidal stretching, where the gravitational potential field from nearby structures distorts the shapes of galaxies along their gravitational field lines (Hirata & Seljak 2004). On the other hand spiral galaxies, acquire angular momentum through linear tidal torquing influencing their orientation with respect to surrounding matter (SCHA¨FER 2009). This dichotomy in the alignment mechanism of elliptical and spiral galaxies in their local environment forms the basis of two main IA models; which are the Linear Alignment (LA) model for ellipticals and the Tidal Torquing model for spirals.1

Intrinsic alignment is of great significance in cosmological studies, especially in the era of precision cosmology and its imprint is detected in cosmological observable, such as the cosmic microwave background (Larsen & Challinor 2016; LEWIS & CHALLINOR 2006), galaxy clustering (Joachimi & Bridle 2010), and most notably, weak gravitational lensing (Mandelbaum

et al. 2006). IA can introduce contamination which can lead to biased estimations of the cosmic shear, which in turn affects the accuracy for cosmological parameter estimation, as is revealed in the works of Kirk et al. (2012).

The Tidal Alignment and Tidal Torquing (TATT) model resulted from the amalgamation of Tidal Alignment and Tidal Torquing theories first suggested by Blazek et al. (2019) to account for the alignment of spiral galaxies as their orientations rely on angular momentum (Lamman et al. 2023). The TATT model is parameterized by essentially four parameters: A1 and η1 defining the amplitude and redshift scaling of the tidal alignment component relevant mostly to the elliptical galaxies and A2 and η2 capturing the higher-order torquing effects for spiral galaxies galaxies.

3. Model Formulation

The intrinsic shape of a galaxy in terms of trace-free tidal tensor sij expanded to second order can be represented as:

$$\gamma_{ij}^{I} = C_1 s_{ij} + b_{\gamma_A} C_1(\delta s_{ij}) + C_2 \left[\sum_{k=0}^{2} \frac{s_{ik} S_{kj} - \frac{1}{3}\delta_{ij} s^2}{2} \right] \tag{1}$$

(Samuroff et al. 2021), where *s* and δ refer to the tidal field and matter over density. Now the amplitude C_1 describing the alignment of galaxies can be written as,

$$C_1(z) = -A_1 \frac{\bar{C}_1 \Omega_m}{D(z)} \left(\frac{1+z}{1+z_0} \right)^{\eta_1} \tag{2}$$

and the tidal torqueing is given by

$$C_2(z) = 5A_2 \frac{\bar{C}_{1\rho c} \Omega_m}{D^2(z)} \left(\frac{1+z}{1+z_0} \right)^{\eta_2} \tag{3}$$

where $\bar{C}_1 = 5 \times 10^{-14} M_e^{-1} h^{-2}$ (Brown et al. 2002) is the constant of normalization and $z_0 = 0.62$ is the pivot redshift (Campos et al. 2023), $D(z)$ is the growth factor of perturbations which is normalized to $(1 + z)$ during matter domination.

4. Methodology

For modeling purposes, we generate datavectors, based on the COCOA model (Miranda et al. 2021) that uses the Cobaya framework (Torrado & Lewis 2021), that mock LSST like data set. These datavectors are modeled in two sets: the first set that ignores higher order terms A_2 and η_2, and the second set that incorporates these. The first set contains 25 datavectors which are unique combinations pertaining to the 5 values of A_1 and η_1 each. These values centered around the fiducial values of 0.7 and -1.7 of A_1 and η_1 respectively. Then we chose 3 values for each of the parameters A_1, η_1, A_2, and η_2, in the same manner as for the simplified model. Their permutations resulted in 81 unique datavectors. The fiducial values we used in our analysis were obtained from Campos et al. (2023).

After obtaining the two sets of datavectors, we carried out statistical analysis to check the fitness of our model and investigate its behavior with changes in the values of the parameters. This was done by calculating the $\Delta\chi^2$ for both the shear and the GGL signals for each of the generated datavectors against a fiducial datavector. To only account for the relevant data we use a mask while populating the covariance matrix whose inverse is used to calculate the $\Delta\chi^2$.

Table 1. Values of the IA parameters and their respective priors.

Parameter	Value	Prior
A_1	0.7	U[−5, 5]
A_2	-1.36	U[−5, 5]
η_1	-1.7	U[−5, 5]
η_2	-2.5	U[−5, 5]
b_{TA}	1.0	U[0, 2]

5. Results

5.1. Analysis with Ignored Higher Order Terms

In Figure 1 we see higher $\Delta\chi^2$ values as A_1 increases or when the η_1 decreases. However, the effect of change in η_1 is less prominent when compared to the change in A1. The $\Delta\chi^2$ displays a similar behavior in the case of GGL with it being consistently higher than that for shear. This implies galaxy-galaxy lensing is more sensitive to changes in A_1 and η_1.

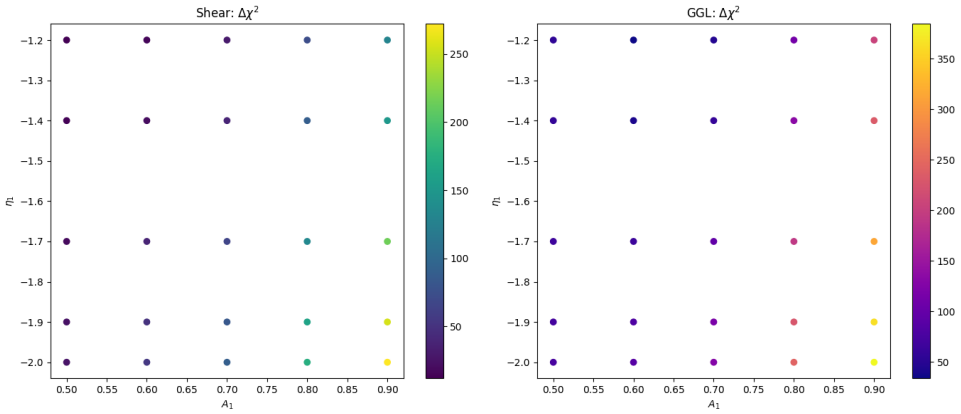

Fig. 1. Scatter plots of $\Delta\chi^2$ for shear and GGL for the simplified model

5.2. Analysis with Higher Order Terms

The results of our analysis with higher order terms for the TATT model are displayed in figures 2, 3, 4, and 5. To study the behaviour of GGL and shear at different scales we take our analysis in two separate avenues:

1. Computing $\Delta\chi^2$ varying the parameters A_2 and η_2 keeping A_1 and η_1 fixed
2. Computing $\Delta\chi^2$ varying the parameters A_1 and η_1 keeping A_2 and η_2 fixed

Upon fixing A_1 and η_1, and varying A_2 and η_2 we see $\Delta\chi^2$ values for GGL are generally higher than that for shear as was seen in the previous case. For the case when we fixed A_1 and η_1, as expected, we see that the $\Delta\chi^2$ tends to increase with more extreme values of A_2 and η_2. This change is more noticeable in the case of A_2. This is consistent with the fact that deviations from fiducial values of the parameters lead to a poorer fit. When we fix A_2 and η_2 the visible trend suggests that the $\Delta\chi^2$ values increase rapidly with changing A_1. The other inference that we can make is that the precision decreases with larger deviations from fiducial values. e.g.- for $A_1 = 0.7$, $\eta_1 = -1.7$ the $\Delta\chi^2$ varies within the range $\in [0.0, -1.6]$. Similarly for $A_1 = 0.8$, $\eta_1 = -2.2$ the $\Delta\chi^2 \in [\sim 15.0, 32.5]$. This leads to the other observation that the $\Delta\chi^2$ for GGL maps a larger range of values when we change the parameter A_1. Similarly, in the case of shear, a larger change $\Delta\chi^2$ is seen for the cases when we vary A_2. The other assertion that can be made is that changes in η_1 and η_2 dominate GGL and shear respectively.

6. Conclusion

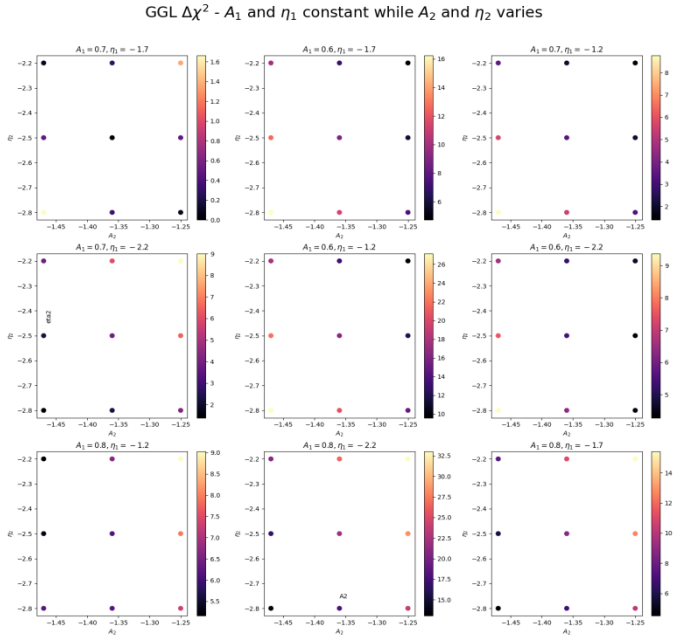

Fig. 2. GGL - $\Delta\chi^2$ with A_1 and η_1 constant

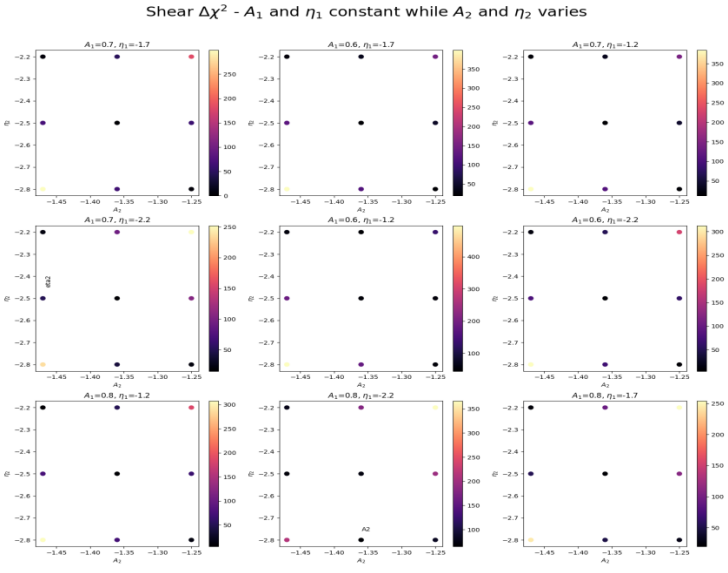

Fig. 3. Shear - $\Delta\chi^2$ with A_1 and η_1 constant

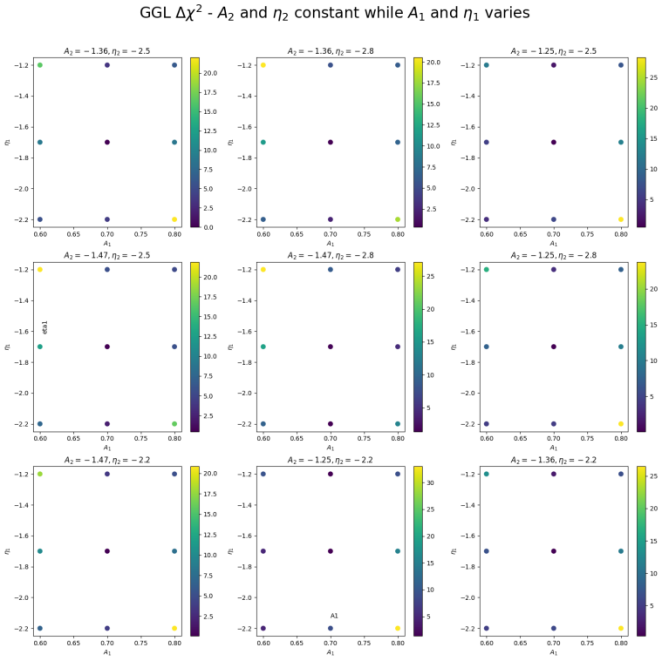

Fig. 4. GGL - $\Delta\chi^2$ with A_2 and η_2 constant

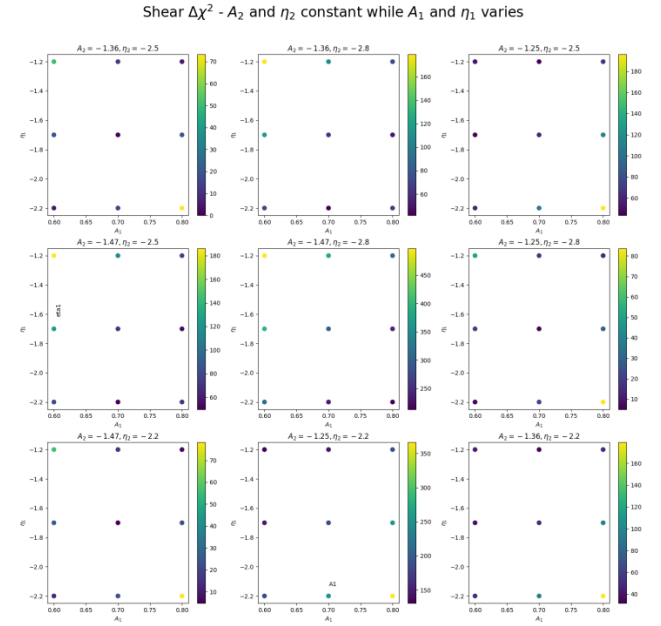

Fig. 5. Shear - $\Delta\chi^2$ with A_2 and η_2 constant

In this work, we investigated the intrinsic alignment of galaxies, by applying the TATT model on a synthetic data set prepared as described in section 4. Initially, we worked with only the linear terms of the intrinsic shape that describes the tidal alignment of galaxies. Then we incorporated the higher order terms that A_2 and η_2, which form the tidal torquing parameter C_2. Then we investigated how our model performs against the standard observational model and how GGL and shear signals react to changing the parameters.

From our results of the $\Delta\chi^2$ analysis, we have concluded that the GGL signal is dominated by the tidal alignment effect while tidal torque dominates the shear signal. We also observe that the amplitudes A_1 for tidal alignment and A_2 for tidal torquing effects carry greater significance compared to the power law indices η_1 and η_2, which describe the redshift evolution of the aforementioned amplitude terms.

References

Bhowmick, A. K., Chen, Y., Tenneti, A., Di Matteo, T., & Mandelbaum, R. 2019, Monthly Notices of the Royal Astronomical Society, 491, 4116–4130, doi: 10.1093/mnras/stz3240

Blazek, J. A., MacCrann, N., Troxel, M., & Fang, X. 2019, Physical Review D, 100, doi: 10.1103/physrevd.100.103506

Brainerd, T. G., Blandford, R. D., & Smail, I. 1996, ApJ, 466, 623, doi: 10.1086/177537

Brown, M. L., Taylor, A. N., Hambly, N. C., & Dye, S. 2002, MNRAS, 333, 501, doi: 10.1046/j.1365-8711.2002.05354.x

Campos, A., Samuroff, S., & Mandelbaum, R. 2023, Monthly Notices of the Royal Astronomical Society, 525, 1885–1901, doi: 10.1093/mnras/stad2213

Doroshkevich, A. G. 1970, Astrophysics, 6, 320, doi: 10.1007/BF01001625

Hirata, C. M., & Seljak, U. 2004, PhRvD, 70, 063526, doi: 10.1103/PhysRevD.70.063526

Joachimi, B., & Bridle, S. L. 2010, Astronomy amp; Astrophysics, 523, A1, doi: 10.1051/0004-6361/200913657

Joachimi, B., Cacciato, M., Kitching, T. D., et al. 2015, Space Science Reviews, 193, 1–65, doi: 10.1007/s11214-015-0177-4

Kiessling, A., Cacciato, M., Joachimi, B., et al. 2015, Space Science Reviews, 193, 67–136, doi: 10.1007/s11214-015-0203-6

Kirk, D., Rassat, A., Host, O., & Bridle, S. 2012, Monthly Notices of the Royal Astronomical Society, 424, 1647–1657, doi: 10.1111/j.1365-2966.2012.21099.x

Lamman, C., Tsaprazi, E., Shi, J., et al. 2023, arXiv e-prints, arXiv:2309.08605, doi: 10.48550/arXiv.2309.08605

Larsen, P., & Challinor, A. 2016, Monthly Notices of the Royal Astronomical Society, 461, 4343–4352, doi: 10.1093/mnras/stw1645

Lewis, A., & Challinor, A. 2006, Physics Reports, 429, 1–65, doi: 10.1016/j.physrep.2006.03.002

Mandelbaum, R. 2018, ARA&A, 56, 393, doi: 10.1146/annurev-astro-081817-051928

Mandelbaum, R., Hirata, C. M., Ishak, M., Seljak, U., & Brinkmann, J. 2006, Monthly Notices of the Royal Astronomical Society, 367, 611–626, doi: 10.1111/j.1365-2966.2005.09946.x

Miranda, V., Rogozenski, P., & Krause, E. 2021, Monthly Notices of the Royal Astronomical Society, 509, 5218–5230, doi: 10.1093/mnras/stab3068

Samuroff, S., Mandelbaum, R., & Blazek, J. 2021, Monthly Notices of the Royal Astronomical Society, 508, 637–664, doi: 10.1093/mnras/stab2520

Scha¨ Fer, B. M. 2009, International Journal of Modern Physics D, 18, 173–222, doi: 10.1142/s0218271809014388

Torrado, J., & Lewis, A. 2021, Journal of Cosmology and Astroparticle Physics, 2021, 057, doi: 10.1088/1475-7516/2021/05/057

Troxel, M. A., & Ishak, M. 2014, arXiv:1407.6990 [astro-ph.CO], doi: 10.48550/arXiv.1407.6990

Wesson, P. S. 1984, A&A, 138, 253